J. Phys. Chem. A **2007,** *111,* 13233−13237

Bonding of CO and NO to NiO(100): a Strategy for Obtaining Accurate Adsorption Energies

Imed Mehdaoui and Thorsten Klüner*

Carl von Ossietzky Universität Oldenburg, Institut für Reine und Angewandte Chemie, Theoretische Chemie and the Center of Interface Science (CIS), Postfach 2503, D-26111 Oldenburg, Germany

Received: July 20, 2007; In Final Form: September 7, 2007

Ab initio studies of the bonding of CO and NO to a NiO(100) surface are presented. As has been shown by Pacchioni et al. (Pacchioni, G.; Di Valentin, C.; Dominguez-Ariza, D.; Illas, F.; Bredow, T.; Klüner, T.; Staemmler, V. *J. Phys.: Condens. Matter* **2004**, *16*, S2497), density functional theory (DFT) fails in predicting accurately the bonding of CO and NO to a NiO(100) surface. In particular, in the case of the NO−NiO(100) system, DFT gives a physically incorrect picture of the bonding. Although the second-order complete active space perturbation theory (CASPT2) method gives qualitatively correct results, still, some uncertainty exists regarding the experimentally predicted value of the adsorption energy. We show that an accurate description of the bonding in the CO−NiO(100) and NO−NiO(100) systems, in fact, represents a challenge to theory, and we will identify the origin of the underestimated bond strength by using different ab initio approaches, and cluster models of systematically increasing size.

I. Introduction

The bonding of small molecules to (transition) metal oxides and the corresponding understanding of photoinduced processes at surfaces are of fundamental interest in many areas of chemistry, physics, and materials science.[1−4] In particular, the accurate description of the bonding of CO and NO to a NiO(100) surface represents a serious challenge to theory.[5−7] On this account, Hoeft has questioned the capability of theoretical methods to describe accurately the bonding of CO, NO, and NH_3 to a NiO(100) surface.[8] Although density functional theory (DFT) is a very effective and widely used tool to study the electronic structure of extended systems, such as metal oxides, via both slab and cluster models, Pacchioni et al. pointed out in a recent study that DFT results are strongly dependent on the exchange-correlation functional used. Especially NO−NiO(100) poses a great challenge, since it is very difficult to treat using DFT methods. Thus, DFT gives a physically incorrect picture of the bonding in the NO−NiO(100) system.[5,6] In cases wherein DFT fails in describing the correct physical nature of such systems, wavefunction-based methods that explicitly include dynamic correlation are essential. Although the CASPT2 method gives results in reasonable agreement with experiment, some uncertainty still exists.[5] In this work, we will present an extended ab initio study of the bonding of CO and NO molecules to a NiO(100) surface using restricted open-shell Hartree−Fock (ROHF), second-order open-shell Møller−Plesset perturbation theory (RMP2), complete active space self-consistent field (CASSCF), complete active space perturbation theory (CASPT2), and coupled cluster approaches and cluster models of systematically increasing size for the NiO(100) surface. Furthermore, we will identify the origin of the discrepancy in former studies in the adsorption energy between theory and experiment.

II. Geometry and Adsorption Energy

To elucidate the origin of the discrepancy between theory and experiment in the adsorption energy of CO and NO adsorbed on a NiO(100) surface, a number of calculations using different levels of theory and cluster models of increasing size, which were embedded in a point charge field (PCF) of about 2900 point charges, were performed. The geometry of the cluster models corresponds to the ideal rock salt structure of bulk NiO with a lattice constant of 4.176 Å.[9] The results summarized in parts A and B of this section have already partially been published in refs 2−4. The adsorption energies have been corrected for the basis set superposition error (BSSE) as proposed by Boys and Bernardi.[10] If not otherwise mentioned, the basis set shown in Table 1 has been used. All calculations on the ROHF, RMP2, CASSCF, and CASPT2 level of theory were performed using the MOLCAS program package,[11] whereas the coupled cluster calculations were performed using the corresponding code implemented in the MOLPRO package of ab initio programs.[12−14] To minimize confusion: Due to the fact that the adsorption energy is negative, in the following paragraphs, an overestimated adsorption energy corresponds to a too-low CO− and NO−NiO(100) bond strength, as compared to experiment. Thus, a decrease in the adsorption energy corresponds to a stronger bond.

A. CO−NiO(100). The geometry of the CO−NiO(100) system was optimized at the RMP2 level using a CO−$NiO_5Mg_{13}^{18+}$/PCF model by pointwise calculation of the six-dimensional potential energy surface around the experimental minimum energy geometry. The coordinates of the cluster atoms have been kept fixed. The $3d_{z^2}$ and $3d_{x^2-y^2}$ orbitals of the Ni atom were singly occupied in a high-spin configuration. In the RMP2 calculation, the C 1s; O 1s; Ni 1s, 2sp, 3sp; and the Mg 1s, 2sp orbitals were excluded from the correlation space. In the minimum energy geometry of the $\tilde{X}^3B_1$ ground state, the C atom is located atop the central Ni atom with the C−O bond parallel to the surface normal, as illustrated in Figure 1. The C−Ni distance of 2.15 Å slightly overestimates the experimental value of 2.07 Å,[8] whereas the C−O bond length of 1.14 Å is in almost perfect agreement with the experimental finding of 1.15 Å.[8]

---

* Corresponding author. E-mail: Thorsten.Kluener@uni-oldenburg.de.

10.1021/jp075703i CCC: $37.00

TABLE 1: Basis Set I Used for the Quantum Chemical Calculations[a−c]

atom type standard basis	extensions
Ni (14s9p5d) → ⟨9s6p4d⟩ of Wachters [16]	+ s ($\zeta = 0.35$) + p ($\zeta = 0.25$) + d ($\zeta = 0.15$) + 2 × f ($\zeta = 2.1; 0.7$)
O (cluster) (9s5p) → ⟨6s3p⟩ of Huzinaga [16]	+ d ($\zeta = 0.4$)[1] + s, p ($\zeta = 0.1; 0.1$)
Mg (10s6p) → ⟨2s1p⟩[2]	
O(CO) (9s5p) → ⟨6s3p⟩ of Huzinaga [16]	+ s ($\zeta = 0.0738$) + p ($\zeta = 0.0597$) + 3 × d ($\zeta = 1.2; 0.4; 0.15$) + f ($\zeta = 0.4$)
C (9s5p) → ⟨6s3p⟩ of Huzinaga [16]	+ s ($\zeta = 0.0440$) + p ($\zeta = 0.03569$) + 3 × d ($\zeta = 0.9; 0.3; 0.1$) + f ($\zeta = 0.3$)
N (9s5p) → ⟨6s3p⟩ of Huzinaga [16]	+ s ($\zeta = 0.0576$) + p($\zeta = 0.0491$) + 3 × d ($\zeta = 0.9; 0.3; 0.1$) + f ($\zeta = 0.3$)

[a] 332 basis functions. [b] For the oxygen ions in the uppermost surface layer only. [c] Exponents and contraction coefficients optimized for $\mathrm{Mg^{2+}}$.

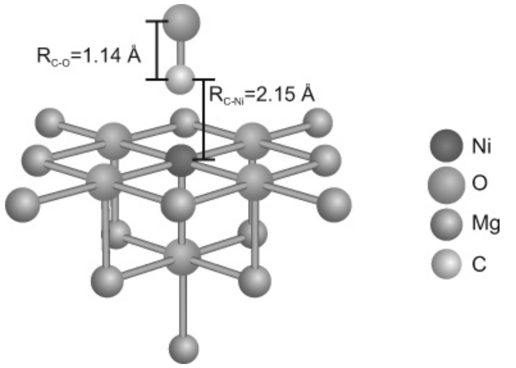

Figure 1. Minimum energy geometry of CO on the $\mathrm{NiO_5Mg_{13}^{18+}}$/PCF cluster in the $\tilde{X}^3B_1$ ground state. The point charge field used is not shown.

TABLE 2: Adsorption Energy of CO on $\mathrm{NiO_5Mg_{13}^{18+}}$/PCF Computed at Different Levels of Theory[a]

method	adsorption energy/eV
ROHF	0.29 (0.21)
RMP2	−0.10 (−0.40)
RMP2[b]	−0.13 (−0.28)
RCCSD	−0.02 (−0.33)
RCCSD(T)	−0.09 (−0.43)
experiment	−0.30

[a] Values without BSSE Correction are in parentheses. [b] Calculations done with the larger ANO basis set shown in Table 3.

TABLE 3: Basis Set II Used for the Quantum Chemical Calculations[a]

atom	contraction	literature
Ni	(21s15p10d6f) → ⟨7s6p5d4f⟩	Pou [17]
O (Cluster)	(10s6p3d) → ⟨5s4p2d⟩	Pierloot [18]
Mg	(13s8p3d) → ⟨3s2p1d⟩	Pierloot [18]
C or N	(14s9p4d3f) → ⟨6s6p3d2f⟩	Widmark [19]
O (CO or NO)	(14s9p4d3f) → ⟨6s6p3d2f⟩	Widmark [19]

[a] 501 basis functions.

Although the geometry of the CO−NiO(100) system is accurately described using this cluster model, some uncertainty exists in the adsorption energy at the RMP2 level, which is −0.10 eV, overestimating the experimental value of −0.30 eV by 0.20 eV. The corresponding interaction energy at the ROHF level is clearly repulsive (0.29 eV), pointing out that dynamic correlation is essential in this system due to the almost entirely electrostatic nature of the CO-cluster interaction. Using a much larger ANO basis set (basis set II; Table 3), the adsorption energy on the RMP2 level decreases to −0.13 eV, in somewhat better agreement with the experiment. Hence, also the BSSE is reduced from 0.30 to 0.15 eV as compared to basis set I. These results are in good agreement with a recent study by Pacchioni et al.[5] A summary of the adsorption energies can be found in Table 2.

Figure 2 presents a correlation diagram of gas-phase CO in the $X^1\Sigma^+$ ground state, the CO−$\mathrm{NiO_5Mg_{13}^{18+}}$/PCF complex in the $\tilde{X}^3B_1$ ground state in the corresponding minimum energy geometry and the $\mathrm{NiO_5Mg_{13}^{18+}}$/PCF cluster in the $\tilde{X}^3B_1$ ground state. After adsorption of the CO molecule onto the $\mathrm{NiO_5Mg_{13}^{18+}}$/PCF cluster, the 5$\sigma$ and 1π orbitals of the CO molecule are pushed downward in energy by ∼1.7 and 0.2 eV, respectively. Conversely, the energy of the d orbitals of the Ni atom are increased in energy by ∼0.3−0.6 eV. Since no bonding orbital is formed between molecular orbitals of the CO molecule and orbitals of the Ni atom, in contrast to the $\tilde{A}^3E$ excited-state of the CO−$\mathrm{NiO_5Mg_{13}^{18+}}$/PCF[4] system, it is conclusive that the interaction is mainly electrostatic in nature. This conclusion is affirmed by calculations on a CO−$\mathrm{Mg_{14}O_5^{18+}}$/PCF adsorbate−substrate complex, wherein the orbital energies of the CO molecule are virtually identical to the CO−$\mathrm{NiO_5Mg_{13}^{18+}}$/PCF system.

A more reliable way of including dynamical correlation on top of a HF calculation is to employ a coupled cluster approach. In these calculations, the C 1s; O 1s; Ni 1s, 2sp, 3sp; and the Mg 1s, 2sp orbitals were not correlated. Using the geometry

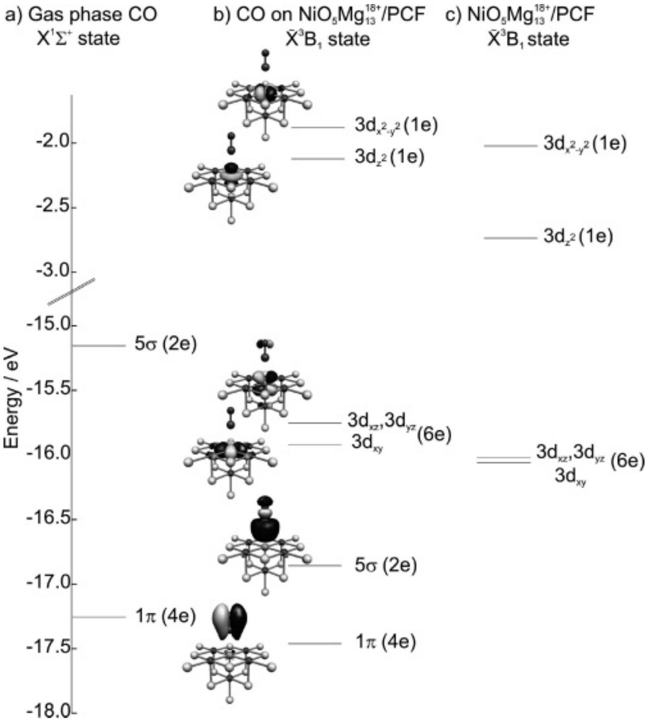

Figure 2. Correlation diagram of (a) gas-phase CO in the $X^1\Sigma^+$ ground state, (b) the CO−$\mathrm{NiO_5Mg_{13}^{18+}}$/PCF complex in the $\tilde{X}^3B_1$ ground state in the minimum energy geometry, and (c) $\mathrm{NiO_5Mg_{13}^{18+}}$/PCF in the $\tilde{X}^3B_1$ ground state. The orbital occupation numbers are shown in parentheses. For the cluster orbitals, only d orbitals of Ni are shown. Images of the orbitals were obtained using the MOLEKEL program.[23,24]

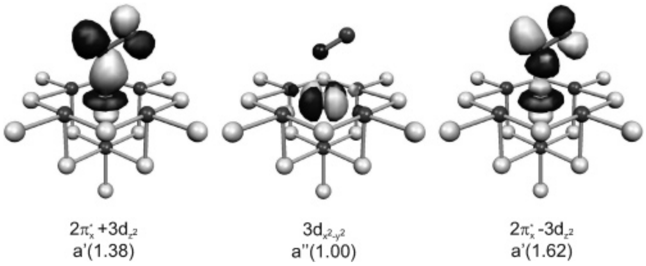

Figure 3. CASSCF(3, 3) active molecular orbitals of the NO−NiO-(100) system in the minimum energy geometry in the $\tilde{X}^2A'$ ground state. The orbital occupation numbers are shown in parnetheses. Images of the orbitals were obtained using the MOLEKEL program.[23,24]

optimized at the RMP2 level, the BSSE corrected adsorption energy is substantially overestimated at the RCCSD level and is only −0.02 eV. Using the RCCSD(T) method, which is known as a very accurate standard method for calculating adsorption energies, the adsorption energy decreases to −0.09 eV, which is almost identical to the RMP2 result, still overestimating the experimental value by about 0.2 eV (Table 2). Note that a geometry optimization at the RCCSD(T) level will yield a slightly increased CO−NiO bond strength but has not been performed due to the high computational cost of such calculations. Since the results of the RCCSD(T) calculations are virtually identical to the results on the RMP2 level, we conclude that the RMP2 method, although in general not as accurate as the RCCSD(T) method, is adequate in predicting accurate adsorption energies. This may be presumably due to a fortuitous cancellation of errors. Consequently, the discrepancy in the adsorption energy may be due to deficiencies inherent to the model system. A systematic study using clusters of different size and composition is discussed in Section III. In addition, the convergence of the adsorption energy as a function of the size of the active space in CASSCF calculations is discussed.

B. NO−NiO(100). In contrast to the CO−NiO(100) system, accurate calculations of the electronic structure of the NO−NiO(100) system are even more involved due to the complicated spin couplings in this system. In fact, this system cannot be described at the ROHF level of theory due to its multiconfigurational character. By means of the CASPT2 method, the geometry of the NO−NiO(100) system was optimized using a NO−$NiO_5Mg_{13}^{18+}$/PCF model, whereas the coordinates of the cluster atoms were kept fixed. The optimization was performed by pointwise calculation of the six-dimensional potential energy surface around the experimental minimum energy geometry. The active space of the preceding CASSCF(3,3) calculation included the singly occupied antibonding $2\pi^*$ orbital of the NO molecule, the singly occupied $3d_{z^2}$ and $3d_{x^2-y^2}$ orbitals of the Ni atom and three active electrons. The active molecular orbitals are shown in Figure 3. In the CASPT2 calculation, the N 1s; O 1s; Ni 1s, 2sp, 3sp; and the Mg 1s, 2sp orbitals were excluded from the correlation space.

In the minimum energy geometry of the $\tilde{X}^2A'$ ground state, the N atom of the NO molecule is located atop the Ni atom with a N−Ni bond length of 1.99 Å, which is somewhat larger than the experimental value of 1.88 Å. The tilt angle between the N−O bond and the surface normal and the N−O bond length are 58° and 1.17 Å, respectively, which is in good agreement with the experimental findings of 59° and 1.12 Å. The theoretical values are summarized in Figure 4. The experimental geometrical parameters can be found in refs 8 and 20. An extensive amount of additional experimental data for the NO−NiO(100) system can be found in ref 21.

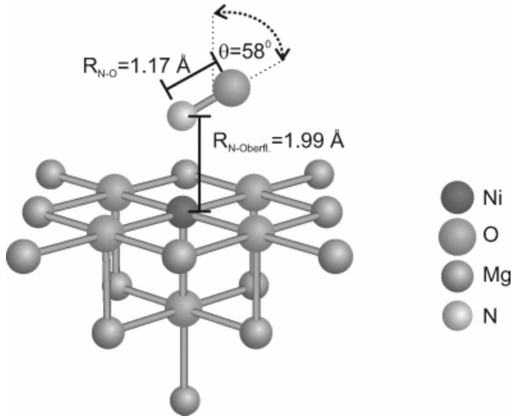

Figure 4. Minimum energy geometry of NO on the $NiO_5Mg_{13}^{18+}$/PCF cluster in the $\tilde{X}^2A'$ ground state. The point charge field used is not shown.

TABLE 4: Adsorption Energy of NO on $NiO_5Mg_{13}^{18+}$/PCF Computed at the CASSCF and CASPT2 Levels of Theory

method	adsorption energy/eV
CASSCF(3,3)	0.46 (0.37)
CASPT2	−0.34 (−0.70)
CASPT2[b]	−0.38 (−0.53)
experiment	−0.57

[b] Values without BSSE correction are in parentheses. [b] Calculations done with the larger ANO basis set shown in Table 3.

The tilted geometry is mainly due to the coupling of the unpaired electron in the antibonding $2\pi^*$ orbital of the NO molecule with the $3d_{z^2}$ orbital of the Ni atom, which yields the formation of a covalent N−Ni bond (indicated by $2\pi_x^* + 3d_{z^2}$ in Figure 3). This results in a somewhat stronger N−Ni bond of −0.34 eV as compared to the CO−NiO(100) system (Table 4). Similarly to the CO−NiO(100) system, the adsorption energy is overestimated by 0.23 eV as compared to the experimental value of −0.57 eV.[22] The corresponding interaction energy on the CASSCF level is, with 0.46 eV, clearly repulsive. In addition, for this system, an ANO basis set (basis set II; Table 3) was used to test the effect of enlarging the basis set by a factor of ∼1.5. Using the ANO basis set, the adsorption energy on the CASPT2 level decreases to −0.38 eV, also in somewhat better agreement with the experimental finding. Attitionally, the BSSE is reduced from 0.36 to 0.15 eV as compared to basis set I. An even larger basis set with a total number of 666 basis functions yielded only a minor improvement in the adsorption energy of −0.02 eV, whereas the BSSE stayed constant. A summary of the adsorption energies can be found in Table 4.

These results are in good agreement with a recent study of Pacchioni et al.,[5] who additionally performed systematic DFT calculations for this system. Not only cluster calculations were performed, but also periodic super-cell calculations. In contrast to the CO−NiO(100) system, no conclusive results could be obtained, and in addition, the wave functions were highly spin-contaminated due to the multiconfigurational character of the NO−NiO(100) system. In principle, multiconfiguration coupled cluster approaches, such as MC-CEPA, may be suitable to treat such systems. Such calculations have already been done by Pacchioni et al.[5] and have therefore not been repeated. Pacchioni et al. showed that the MC-CEPA method using different basis sets and cluster models yields only very small binding energies of only −0.05 to −0.10 eV.

Due to the very similar characteristics to the CO−NiO(100) system, the lack in predicting accurate adsorption energies might be due to deficiencies in the model systems used so far in this

TABLE 5: Adsorption Energy of CO on $NiO_5Mg_{13}^{18+}$/PCF for Different Active Spaces in the CASSCF Calculations[a]

	adsorption energy/eV		
active space	(8, 7)	(12, 10)	(18, 13)
CASSCF	0.32	0.30	0.30
CASPT2	−0.05	−0.06	−0.07
experiment		−0.30	

[a] All values have been corrected for the BSSE.

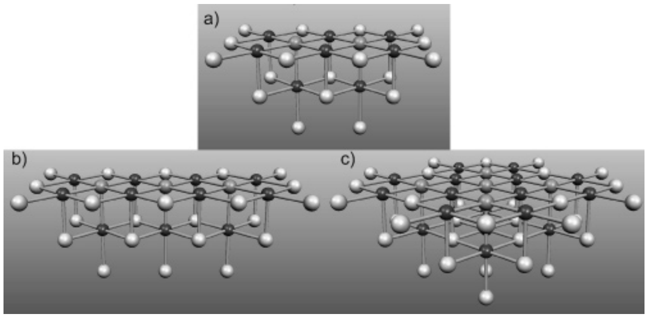

Figure 5. Geometry of the (a) $Ni_2O_8Mg_{18}^{24+}$/PCF, (b) $Ni_3O_{11}Mg_{23}^{30+}$/PCF, and (c) $Ni_5O_{17}Mg_{33}^{42+}$/PCF cluster. The point charge fields used are not shown. Illustrations were obtained using the MOLEKEL program.[23,24]

and similar studies. Therefore, a systematic study using cluster models of different sizes has been performed for both adsorbate-substrate-systems as discussed in the next paragraph.

III. Convergence of the adsorption energy

A. CO−NiO(100). To provide a first indication of the discrepancy between theory and experiment, CASSCF and CASPT2 calculations in which the active space in the CASSCF calculations is systematically increased were performed. The results are summarized in Table 5. Using an active space of (8, 7), which in addition to the $3d_{z^2}$ and $3d_{x^2-y^2}$ orbitals of Ni includes the doubly occupied 1π and 5σ and the unoccupied $2\pi^*$ antibonding orbitals of the CO molecule, the adsorption energy on the CASPT2 level is increased to −0.05 eV. Augmenting the active space by the whole valence space of the CO molecule (12, 10), the adsorption energy decreases to −0.06 eV. The largest active space (18, 12) includes in addition to the whole valence space of the CO molecule all d orbitals of the Ni atom, which yields a slightly decreased adsorption energy of −0.07 eV, almost as large as the adsorption energy obtained using the RMP2 method (Table 2). This led us to deduce that using the RMP2 method is reasonable to correctly describe the bonding in the CO−NiO(100) system.

In a recent study, Pacchioni et al. pointed out that DFT calculations using a periodic super-cell and a small cluster model with only one Ni atom give virtually the same result and differ by only 0.02 eV.[5] This led to the conclusion that a small cluster model accurately describes the bonding of CO on NiO(100). To test the validity of this conclusion for wavefunction-based methods, wherein dynamical correlation is explicitly treated, a series of calculations were performed with clusters of systematically increasing size and different numbers of Ni atoms. The geometry of these model systems corresponds to the ideal rock salt structure of bulk NiO and is presented in Figure 5. All calculations were performed with all Ni d electrons in high-spin configuration to minimize convergence problems due to the large number of possible complex spin couplings. The results for all cluster models used for the calculations are shown in Table 6. These results illustrate that for each increase in the cluster size and additional Ni atom, the adsorption energy at the RMP2 level linearly decreases by about −0.025 eV. Thus, the adsorption energy for CO on $Ni_5O_{17}Mg_{33}^{42+}$/PCF, the largest cluster model, is −0.20 eV, much closer to the experimental finding. A further calculation with a cluster model of the same size but only one Ni atom, a $NiO_{17}Mg_{37}^{42+}$/PCF cluster, gives a CO−NiO(100) bond strength of only −0.11 eV, revealing that although the bonding is mainly a local effect, the small effects of the neighboring Ni atoms add to a substantial decrease in the adsorption energy. Although properties such as the geometry of the CO−NiO(100) system can already be described accurately by a small CO−$NiO_5Mg_{13}^{18+}$/PCF cluster on the RMP2 level, a very accurate description of the bonding necessitates a much larger cluster model, which also considers neighboring Ni atoms of the corresponding adsorption side. Interestingly, the CO-cluster interaction energy at the ROHF level is virtually independent of the cluster size, pointing out that the inclusion of dynamic correlation is essential to get the correct convergence behavior of the adsorption energy as a function of cluster size.

TABLE 6: Adsorption Energy of CO on NiO(100) Computed at the ROHF and RMP2 Level for Different Cluster Sizes[a]

	adsorption energy/eV	
cluster model	RMP2	ROHF
CO−$NiO_5Mg_{13}^{18+}$/PCF	−0.10 (−0.40)	0.29 (0.21)
CO−$Ni_2O_8Mg_{18}^{24+}$/PCF	−0.12 (−0.43)	0.29 (0.21)
CO−$Ni_3O_{11}Mg_{23}^{30+}$/PCF	−0.15 (−0.46)	0.28 (0.21)
CO−$Ni_5O_{17}Mg_{33}^{42+}$/PCF	−0.20 (−0.54)	0.27 (0.20)
CO−$NiO_{17}Mg_{37}^{42+}$/PCF	−0.11 (−0.52)	0.30 (0.20)
experiment	−0.30	

[a] Values without BSSE correction are in parentheses.

TABLE 7: Adsorption Energy of NO on NiO(100) Computed at the CASSCF and CASPT2 Level for Different Cluster Sizes[a]

	adsorption energy/eV	
cluster model	CASPT2	CASSCF($2n+1,2n+1$)
NO−$NiO_5Mg_{13}^{18+}$/PCF	−0.34 (−0.70)	0.46 (0.37)
NO−$Ni_2O_8Mg_{18}^{24+}$/PCF	−0.38 (−0.74)	0.46 (0.37)
NO−$Ni_3O_{11}Mg_{23}^{30+}$/PCF	−0.41 (−0.79)	0.46 (0.37)
experiment	−0.57	

[a] n is the number of Ni atoms in the corresponding cluster models; values without BSSE correction are in parentheses.

B. NO−NiO(100). Similar to the CO−NiO(100) system, the convergence of the adsorption energy as a function of cluster size has been investigated for NO−NiO(100). Due to the lower symmetry of this system and, thus, higher computational effort needed for the computations, calculations only up to a $Ni_3O_{11}Mg_{23}^{30+}$/PCF model could be performed. The geometry of these model systems corresponds to the ideal rock salt structure of bulk NiO. The cluster models are illustrated in Figure 5. The active space in the CASSCF calculations included the $3d_{z^2}$ and $3d_{x^2-y^2}$ orbitals of all Ni atoms and the singly occupied $2\pi^*$ orbital of the N atom, which yields an active space of ($2n + 1$, $2n + 1$), where n is the number of Ni atoms. In the CASPT2 calculations, the N 1s; O 1s; Ni 1s, 2sp, 3sp; and the Mg 1s, 2sp orbitals were excluded from the correlation space. As can be seen from Table 7, for each increase in the cluster size, the adsorption energy decreases by about −0.035 eV, which yields a stronger N−Ni bond. The adsorption energy for the largest cluster ($Ni_3O_{11}Mg_{23}^{30+}$/PCF) is −0.41 eV. Due to the characteristics that are similar to the CO−NiO(100) system, extrapolation to an adsorption energy of −0.48 eV for a $Ni_5O_{17}Mg_{33}^{42+}$/PCF cluster model seems adequate and is in much better agreement with the experimental finding of −0.57 eV, as compared to the smaller model systems. From these results, it can be concluded that the discrepancy between theoretical and experimental adsorption energies in former studies can be traced back to deficiencies inherent in the methods and in the cluster models used so far: the cluster models were too small to predict very accurate interaction energies or a too small number of Ni atoms has been used.

IV. Conclusion

In conclusion, an extended ab initio study of the bonding of CO and NO on NiO(100) has been presented. The corresponding interaction energies have been investigated at the ROHF, RMP2, CASSCF, CASPT2, and RCC level of theory using clusters of systematically increasing size, which are embedded in a field of point charges. Although the geometry of these systems can accurately be described when using a small cluster model with only one Ni atom, some uncertainty exists concerning the adsorption energies, which led to a recent debate concerning the capability of current theoretical methods to accurately describe the bonding of CO and NO to a NiO(100) surface. In contrast to this, we clearly demonstrate that a very accurate description can be obtained at the RMP2 and CASPT2 levels with both large clusters and a sufficiently large number of Ni atoms. Since results on the DFT level strongly depend on the functional used and, moreover, may give a physically incorrect picture, this shows the importance of systematically improvable ab initio methods that explicitly account for both dynamical correlation effects and the multiconfigurational character of such systems in combination with cluster models.

References and Notes

(1) Saalfrank, P. *Chem. Rev.* **2006**, *106*, 4116.

(2) Kröner, D.; Mehdaoui, I.; Freund, H.-J.; Klüner, T. *Chem. Phys. Lett.* **2005**, *415*, 150.

(3) Mehdaoui, I.; Kröner, D.; Pykavy, M.; Freund, H.-J.; Klüner, T. *Phys. Chem. Chem. Phys.* **2006**, *8*, 1584.

(4) Mehdaoui, I.; Klüner, T. *Phys. Rev. Lett.* **2007**, 9*8*, 037601.

(5) Pacchioni, G.; Di Valentin, C.; Dominguez-Ariza, D.; Illas, F.; Bredow, T.; Klüner, T.; Staemmler, V. *J. Phys.: Condens. Matter* **2004**, *16*, S2497.

(6) Valentin, C. D.; Pacchioni, G.; Bredow, T.; Dominguez-Ariza, D.; Illas, F. *J. Chem. Phys.* **2002**, *117*, 2299.

(7) Pacchioni, G.; Cogliandro, G. *Surf. Sci.* **1991**, *255*, 344.

(8) Hoeft, J. T.; Kittel, M.; Polcik, M.; Bao, S.; Toomes, R. L.; Kang, J. H.; Woodruff, D. P.; Pascal, M.; Lamont, C. L. A. *Phys. Rev. Lett.* **2001**, *87*, 086101.

(9) Newman, R.; Chrenko, R. M. *Phys. Rev.* **1959**, *114*, 1507.

(10) Boys, S. F.; Bernardi, F. *Mol. Phys.* **1970**, *19*, 553.

(11) Karlström, G.; Lindh, R.; Malmqvist, P.-Å.; Roos, B. O.; Ryde, U.; Veryazov, V.; Widmark, P.-O.; Cossi, M.; Schimmelpfennig, B.; Neogrady, P.; Seijo, L. *Comput. Mater. Sci.* **2003**, *28*, 222.

(12) Werner, H.-J.; Knowles, P. J.; Lindh, R. F.; Manby, R.; Schütz, M.; Celani, P.; Korona, T.; Rauhut, G.; Amos, R. D.; Bernhardsson, A.; Berning, A.; Cooper, D. L.; Deegan, M. J. O.; Dobbyn, A. J.; Eckert, F.; Hampel C.; Hetzer, G.; Lloyd, A. W.; McNicholas, S. J.; Meyer, W.; Mura, M. E.; Nicklass, A.; Palmieri, P.; Pitzer, R.; Schumann, U.; Stoll, H.; Stone, A. J.; Tarroni, R.; T. Thorsteinsson. MOLPRO, version 2006.1; a package of ab initio programs.

(13) Knowles C. H. P. J.; Werner, H.-J. *J. Chem. Phys.* **1993**, *99*, 5219.

(14) Knowles, C. H. P. J.; Werner, H.-J. *J. Chem. Phys.* **2000**, *112*, 3106.

(15) Wachters, A. *Chem. Phys.* **1965**, *42*, 1033.

(16) Huzinaga, S.; Roos, B. *Theor. Chim. Acta* **1995**, *92*, 149.

(17) Pou-Amerigo, R.; Merchan, M.; Widmark, P.-O.; Roos, B. *Theor. Chim. Acta* **1995**, *92*, 149.

(18) Pierloot, K.; Dumez B.; Widmark, P.-O.; Roos, B. O. *Theor. Chim. Acta* **1995**, *90*, 87.

(19) Widmark, P.-O.; Malmqvist, P.-Å.; Roos, B. O. *Theor. Chim. Acta* **1990**, *77*, 291.

(20) Lindsay, R.; Baumgärtel, P.; Terborg, R.; Schaff, O.; Brandshaw, A. M.; Woodruff, D. P. *Surf. Sci.* **1999**, *425*, L401.

(21) Kuhlenbeck, H.; Odörfer, G.; Jaeger, R.; Illing, G.; Menges, M.; Mull, T.; Freund, H.-J.; Pöhlchen, M.; Staemmler, V.; Witzel, S.; Scharfschwerdt, C.; Wennemann, K.; Liedtke, T.; Neumann, M. *Phys. Rev. B: Condens. Matter Mater. Phys.* **1991**, *43*, 1969.

(22) Wichtendahl, R.; Rodriguez-Rodrigo, M.; Härtel, U.; Kuhlenbeck, H.; Freund, H.-J. *Surf. Sci.* **1999**, *423*, 90.

(23) Flükiger, P.; Lüthi, H. P.; Portmann, S.; Weber, J. MOLEKEL 4.3. Swiss Center for Scientific Computing, Manno, Switzerland, 2000−2002.

(24) Portmann, S.; Lüthi, H. P. Chimia **2000**, *54*, 766.